Assessment of soil erosion over six decades in a long-term experiment using fallout 137Cs and rusle : a South American case study

Marcos Tassano, Mirel Cabrera, Joan Gonzalez, Mario Perez-Bidegain, Olivier Evrard, Kathrin Grahmann, J. Andrés Quincke

Land Degradation & Development

WILEY

RESEARCH ARTICLE OPEN ACCESS

Assessment of Soil Erosion Over Six Decades in a Long-Term Experiment Using Fallout ^{137}Cs and RUSLE: A South American Case Study

Marcos Tassano[1] | Mirel Cabrera[1] | Joan Gonzalez[1] | Mario Perez-Bidegain[2,3] | Olivier Evrard[4] | Kathrin Grahmann[5] | J. Andrés Quincke[3]

[1]Laboratorio de Radioquímica, Centro de Investigaciones Nucleares, Facultad de Ciencias, Universidad de la República, Montevideo, Uruguay | [2]Soil and Water Department, Faculty of Agronomy-UdelaR, Universidad de la República, Montevideo, Uruguay | [3]National Agricultural Research Institute, La Estanzuela, Colonia, Uruguay | [4]Laboratoire Des Sciences du Climat et de L'environnement (LSCE/IPSL), Université Paris-Saclay, UMR 8212 (CEA-CNRS-UVSQ), Gif-sur-Yvette, France | [5]Leibniz Centre for Agricultural Landscape Research (ZALF), Müncheberg, Germany

Correspondence: Kathrin Grahmann (kathrin.grahmann@zalf.de)

Received: 6 August 2025 | **Revised:** 12 January 2026 | **Accepted:** 7 February 2026

Keywords: crop pasture rotation | deposition | radionuclides Cs137 | RUSLE | soil loss | tillage

ABSTRACT

Soil erosion remains a major global concern affecting agricultural productivity and land sustainability. This study investigates the magnitude and variability of soil erosion in a long-term experiment (LTE) established in 1963 in Colonia, Uruguay, aiming to compare the performance of the ^{137}Cs tracer technique and the RUSLE model across different crop rotations. We hypothesized that pasture inclusion into rotations reduces soil erosion compared to continuous cropping, regardless of the model. Four contrasting LTE treatments were selected: continuous cropping without fertilization, continuous cropping with fertilization, and two crop-pasture rotations with 33% or 50% time under pasture. Each plot had a size of 25 × 200 m positioned along a hillslope and was sampled at six sampling points along a transect from the hilltop towards the footslope. Soil erosion was assessed using two methods: (1) the ^{137}Cs technique, estimating net soil redistribution based on deviations from a reference site, and (2) the RUSLE model, calibrated with national agronomic and climatic data. The ^{137}Cs method showed erosion rates from −73 to +51 Mg ha^{-1} year^{-1}, with accumulation at footslopes and highest losses in eroded gullies under unfertilized continuous cropping. RUSLE predicted losses from −1 to −20 Mg ha^{-1} year^{-1}, based on sheet erosion assumptions. The comparison was limited to five sampling points where erosion processes were dominant and compatible with RUSLE assumptions. Nevertheless, results confirmed that crop-pasture rotations substantially reduced erosion and preserved soil over six decades. We conclude that integrating pastures into rotations is an effective erosion control strategy in sloping agricultural systems and helps maintain long-term productivity.

1 | Introduction

The expansion of agricultural production and land cover change in South America, especially in the Pampa biome, has caused significant environmental impacts, affecting the sustainable use of soil and water resources (Foucher et al. 2023). Agricultural intensity influences soil redistribution, leading to varying erosion and deposition processes (FAO 2019). In Uruguay, concerns over water erosion have a long history (Zurbriggen et al. 2020), with an estimated 30% of agricultural land already affected by erosion in the 1960s (Cayssials et al. 1978). Efforts to improve sustainability started during the Green Revolution with the implementation of crop-pasture systems (termed Crop-Pasture Rotation, CPR), followed by the widespread adoption of no-tillage in the early 1990s (García-Préchac et al. 2004). However, these sustainable practices have gradually been replaced by intensive, continuous cropping systems, with reduced pasture integration

and increased summer crop cultivation, especially soybean (*Glycine max*). Updated assessments showed that 30.1% of Uruguay's territory still suffered from erosion in the early 2000s (MGAP-MVOTMA 2005). In response, Uruguay revised its national soil conservation policies in 2008, requiring crop production farms over 100 ha to submit mandatory soil use and management plans (Perez-Bidegain et al. 2018). The implementation of these plans resulted in a substantial reduction of erosion rates, from 10 Mg ha^{-1} year^{-1} prior to the law to approximately 3 Mg ha^{-1} year^{-1} in recent years (Dell'Acqua and Beretta-Blanco 2020).

Long-term experiments (LTE) are highly suitable to understand how land use changes modify the dynamics in biochemical and geophysical processes over decades, which has lasting consequences for soil erodibility. The long-term beneficial effects of CPR include the improvement of soil structure and soil water holding capacity, and thus, overall improved soil physical properties, which contribute to increased water infiltration during intense rainfall events (Franzluebbers and Gastal 2018). Those positive soil quality changes are primarily driven by soil organic carbon (SOC) derived from pasture root biomass, which acts as a key controlling factor of soil erosion in degraded soils where SOC has declined (Ernst and Siri-Prieto 2009; Ernst et al. 2018). However, detecting and quantifying SOC changes and thus soil erodibility requires decades due to the slow and gradual nature of SOC changes in response to agricultural management (Smith 2004). For the LTE studied here, topsoil SOC was 19% higher in a crop-pasture rotation (21.2 g kg^{-1}) compared to continuous fertilized agriculture (17.6 g kg^{-1}) after 55 years of annual samplings (Grahmann et al. 2020).

Several methodologies exist to estimate soil erosion. The Universal Soil Loss Equation (USLE) (Wischmeier and Smith 1978) and its revised version (RUSLE, Renard et al. 1991) are widely used to plan and assess the effects of soil erosion on agricultural productivity (Alewell et al. 2019). In its standard form, the USLE is applied to uniform slopes over large areas that share parameterizable factors such as land use, soil type, or conservation practices. In Uruguay, the USLE and RUSLE models were validated and adapted to national conditions (García-Préchac and Durán 1998; García-Préchac et al. 2016, 2017) and consequently used for the mandatory soil use and management plans through a national software tool (EROSION 6.0), which is continuously updated (Pérez Bidegain et al. 2022).

The use of environmental radionuclides like Cesium (^{137}Cs) and the calculation of their inventories in soil profiles collected at contrasting sites (i.e., reference, erosion and accumulation sites) before converting them into redistribution rates is another widely used method in soil erosion research to determine erosion/accumulation rates (Zapata 2003; Soto and Navas 2008; Walling et al. 2011). The use of radioisotope methods for soil erosion studies has been in the spotlight of ongoing scientific discussions (García-Ruiz et al. 2015). However, in Uruguay the ^{137}Cs method has been successfully applied to estimate the rate of erosion on slopes (Tassano et al. 2021) and small watersheds (Alonso et al. 2012; Cabrera et al. 2023), thereby demonstrating the usefulness and accuracy of ^{137}Cs as an indicator of land redistribution and erosion rates.

However, most studies using fallout radionuclides (FRNs) have focused on field-scale applications and rarely compared long-term annual erosion rates derived from the experimental ^{137}Cs approach with those estimated using RUSLE (Chen et al. 2023; Čupić et al. 2025). In the ^{137}Cs method, soil inventories measured by gamma spectrometry are converted into mean annual erosion rates (Mg ha^{-1} year^{-1}) using the Mass Balance Model, which accounts for radioactive decay (year^{-1}), a constant relaxation mass depth (kg m^{-2}), a particle size correction factor, and a known regional fallout input. This framework allows reconstruction of soil redistribution rates over approximately the last 60 years since the peak fallout in South America (1964–1972) and assessment of land-use impacts on erosion dynamics (Walling et al. 2011; Chaboche et al. 2021, 2022; Tassano et al. 2025). Among the few erosion studies that applied plot-scale experimentation in LTE (Porto et al. 2022), the focus on agricultural land use change was rare (e.g., Ritchie and Rasmussen 2000), whilst no study was found that assessed the erosion reduction potential of CRP in the long-term.

Therefore, this study aimed to (1) estimate soil erosion using the nuclear tracer ^{137}Cs in a long-term experiment (LTE) initiated in 1963 in contrasting crop rotations; and (2) compare the results of various ^{137}Cs conversion models with validated RUSLE soil erosion estimates for Uruguay. For the first time, the oldest cropping experiment in Latin America was intensively sampled to quantify six decades of soil redistribution by combining ^{137}Cs isotope tracing with the validated national RUSLE model.

2 | Material and Methods

2.1 | Study Area and Long-Term Experiment

The study area is located near Colonia, Uruguay, at the National Institute for Agricultural Research (INIA) La Estanzuela (lat. 34°20′S, long. 57°41′W, 66 m a.s.l.). The area is characterized by a humid subtropical climate (Cfa, Köppen–Geiger classification) with a mean annual rainfall of 1125 mm and a yearly baseline evapotranspiration of approximately 1180 (±143) mm over the last 55 years (Grahmann et al. 2020). The mean maximum monthly temperature ranges from 15°C in winter to 28°C in summer, and the mean monthly minimum temperature ranges from 6°C in winter to 17°C in summer (Baethgen et al. 2021). The soil at the experimental site is classified as a Haplic Phaeozem (Vertic, Eutric; FAO IUSS Working Group WRB 2022) or as a Smectic Vertic Argiudoll (USDA Soil Taxonomy, Soil Survey Staff 2022). The slope is 2.5%–3.0%, and the topsoil (0–15 cm) texture is a silty clay loam (56% silt, 35% clay, 9% sand).

This study was carried out in a LTE established in 1963, which is concurrent with the onset of peak radioactive fallout in the Southern Hemisphere (Chaboche et al. 2022). A comprehensive description of the LTE history and design is provided in Supporting Information (Text S1, Table S1) and (Grahmann et al. 2020). Four treatments were selected in this study: continuous agriculture without fertilization (CA0), continuous agriculture with mineral fertilizer application (CA+), CPR with 50% crops and 50% pasture (50%P), and CPR with 66% crops and 33% pasture (33%P) using single transects in one plot each (CA+,

33%P, 50%P), but two plots across the first (1CA0) and second (2CA0) block for CA0.

2.2 | Soil Sampling and Laboratory Analysis

To determine the ^{137}Cs reference inventory, six sites within a 10 km radius of the LTE were surveyed, ensuring similar soil and geological characteristics to minimize variability from precipitation-driven fallout. The selected reference site, 3 km away from the LTE within the same drainage basin (lat. 34°20′24.0″S, long. 57°41′25.1″W, 66 m a.s.l.), provided six pooled samples (2.5 cm intervals to 35 cm depth) and nine individual profiles. Fine 2.5 cm increments ensured accurate identification of (i) the deepest detectable ^{137}Cs layer, (ii) the effective plow depth inferred from the ^{137}Cs distribution, and (iii) erosion and accumulation processes occurring within the upper soil layers. The average of these samples, with their coefficient of variation (CV%), defined the reference inventory (Figure 2).

For five LTE plots, soil samples were collected along a systematic transect with six points (5, 40, 80, 120, 160, 200 m), using a hydraulic corer (4 cm diameter). At each point, six stratified samples were taken (2.5 cm intervals), with depths ranging from 30 to 100 cm depending on erosion or accumulation conditions. No sampling has been conducted at 5 m under 33%P due to its location at the edge of the catchment, where water flow reverses direction. In total, 470 samples were collected across all plots (e.g., reference site $n = 76$, CA+ $n = 87$). Samples were dried (40°C, 48 h), sieved (2 mm), and stored in 250 mL Marinelli beakers.

Measurements were conducted at the "Laboratorio de Radioquímica, Centro de Investigaciones Nucleares, Facultad de Ciencias, UdelaR" using a high-purity germanium detector (HPGe, 20% efficiency at 1332 keV). ^{137}Cs activity was measured at 661.5 keV (1.62% efficiency) with a minimum detectable concentration of 0.04 Bq kg^{-1}. Measurement precision ranged from ±5% to 10% (95% confidence level), and all data were decay-corrected to January 1, 2020.

2.3 | ^{137}Cs Conversion Models

Several models convert ^{137}Cs inventories (Bq m^{-2}) into erosion or deposition rates (Mg ha^{-1} year^{-1}) for plowed and unplowed soils (Arata et al. 2016; Gharbi et al. 2020; He and Walling 1997; Soto and Navas 2008; Walling et al. 2011). In this study, the Proportional Model, Mass Balance Model II (MBM II), and Mass Balance Model III (MBM III) were applied, as they account for fallout behavior and tillage-induced redistribution (Walling and He 1999; Walling et al. 2002, 2011, 2014). MBM III, in particular, allows the separation of tillage from water erosion. Given that LTE plots are oriented across the slope, erosion-dominant points with minimal deposition were selected for analysis and compared to RUSLE outputs. Model parameters, such as tillage depth, tillage constant, relaxation mass depth, and slope gradients, were carefully estimated. Common parameters applied across all sites included a plow layer mass depth of 167.6 kg m^{-2}, a reference profile distribution parameter (H_0) of 60.6 kg m^{-2} and a mass relaxation depth of 6.2 kg m^{-2}. No particle size corrections were necessary (correction factor = 1), indicating comparable soil texture characteristics across sampling locations.

Site-specific parameterization varied among the five study plots (33%P, 1CA0, CA+, 50%P, and 2CA0), sampled in 2020 (33%P) and 2021 (remaining plots). Agricultural tillage was assumed to have started in 1954 in all plots. The proportionality factor (P), which relates cumulative ^{137}Cs redistribution to net soil loss or gain, ranged from 0.40 to 0.51 depending on local cultivation intensity and landscape position. Ploughing constants, representing the annual rate of vertical soil mixing within the cultivated layer, varied from 21 to 75.5 kg m^{-2} year^{-1} among plots, reflecting differences in tillage practices, equipment type, and land management history. These site-specific parameters were calibrated to account for local pedological and agronomic conditions affecting ^{137}Cs vertical distribution and lateral transport (Walling and He 1999; Walling et al. 2002, 2011, 2014). Additionally, the MODERN model (Arata et al. 2016), applicable to both plowed and no-till systems, estimates erosion by comparing disturbed site inventories to a reference profile. It adjusts for plowing by redistributing activity evenly above the plow layer and, unlike mass balance models, does not require a transect-based sampling scheme, allowing for greater spatial flexibility. A MATLAB program in GNU Octave version 5.1 was used to apply the MODERN model, which was supplied by: https://adam.unibas.ch/goto_adam_file_641865_download.html.

2.4 | RUSLE Soil Erosion Estimation

EROSION 6.0 software (García-Préchac et al. 2016) was used to apply RUSLE in the selected treatments and plots. Two erosion rate estimations were computed per sampling point taking the R factor (rainfall erosivity in MJ mm ha^{-1} h^{-1} year^{-1}) as the minimum (RUSLE min) and mean (RUSLE mean) of the moving average over 20-year periods based on meteorological data from the INIA weather station (since 1965–2020). The meteorological station is situated 3 km from the LTE and 0.3 km from the reference site. The K factor (soil erodibility) was considered 0.023 Mg h MJ^{-1} mm^{-1} and corresponds to the Vertic Argiudoll at the LTE retrieved from the soil survey map of Uruguay (Altamirano et al. 1976). The P factor (support practices) was set to 1 as tillage operations were conducted from up to downhill. Values for the C factor (cover and management) were calculated for each rotation system and LTE period and weighted by the number of years in the respective period (Table S2). Finally, LS (topographic factor) was calculated for each point by taking the average slope associated with the distance from the beginning of the plot (topographically the highest point) to the point of interest. The base maps were obtained through the IDEuy portal (Infraestructura de Datos Espaciales del Uruguay) (https://visualizador.ide.uy/).[1] Digital elevation data were also extracted from the IDEuy digital terrain model with a point-to-point accuracy of 2.5 m.

2.5 | Statistical Analysis

Statistical analyses and data visualizations were conducted using dedicated scientific libraries within Spyder v. 4.1.5

(Raybaut 2009), an integrated development environment for Python v. 3.8.5 (Python Software Foundation; Hunter 2007; McKinney 2010; Harris et al. 2020; Virtanen et al. 2020). Data normality and homogeneity of variances were evaluated using the Shapiro–Wilk and Levene's tests, respectively. Variables that met normality and homoscedasticity assumptions ($p > 0.05$) were analyzed using Pearson's correlation coefficient, while Spearman's rank correlation was applied otherwise. Confidence intervals (95%) were calculated only for MBM II erosion estimates, as this approach allows explicit propagation of analytical uncertainty by incorporating ±1 standard error of measured ^{137}Cs activities into the mass balance calculations. In contrast, RUSLE provides deterministic estimates without an intrinsic error structure. Statistical significance was defined at $p < 0.05$.

2.6 | Classification of Sediment Processes

Sampling points were classified to support the interpretation of soil redistribution patterns derived from ^{137}Cs data. The classification is diagnostic and process-oriented, and it is used to contextualize the obtained quantitative erosion rates. Each point was categorized based on field observations, topographic position, vertical ^{137}Cs depth profiles, and total ^{137}Cs inventories relative to the reference site. Four categories were defined: Erosion (reduced inventories and truncated profiles), Transition (mixed export–import signatures), Deposition (inventories exceeding the reference and deeper ^{137}Cs penetration), and Gully (points affected by concentrated flow erosion with highly disturbed profiles).

3 | Results

3.1 | Soil Erosion Estimation Using ^{137}Cs

Among the analyzed reference sites, only one displayed an exponential decay pattern of ^{137}Cs with depth. The reference site inventory was 367.1 ± 15.9 Bq m^{-2} with a CV of 8.7% ($n = 9$) (Figure 2), a value that is consistent with previously reported inventory levels measured during the nuclear fallout period of the 1950s–1970s in Buenos Aires, located approximately 65 km away in a straight-line distance (Tassano et al. 2025). A summary of soil redistribution rates for each sampled plot and different models is provided in Table 1.

TABLE 1 | Annual net soil redistribution rates (Mg ha^{-1} year^{-1}) estimated using different ^{137}Cs-based conversion models (MBM II, MBM III, PM, and MODERN) and compared with RUSLE-derived erosion rates under minimum and mean rainfall erosivity conditions.

	1CA0	2CA0	CA+	33%P	50%P
Net erosion (Mg ha^{-1} year^{-1})					
MBMII	−15.2	−5.9	−1.1	−1.1	1.1
MBMIII	−15.4	−5.9	−1.5	−1.2	1.3
PM	−11.4	−5.2	−1.1	−1.1	1.3
MODERN	−20.1	−10.5	−6.7	0.8	−0.2
RUSLE (min. R)	−11.6	−10.7	−10.6	−5.7	−5.6
RUSLE (mean R 1963–2020)	−14.8	−13.6	−13.6	−7.2	−7.1
RUSLE (mean R 1963–1983)	−21.4	−19.7	−21.3	−8.2	−9.3
MBM II Gross erosion (Mg ha^{-1} year^{-1})	−24.4	−11.3	−7.4	−3.5	−2.8
MBM II Sediment delivery ratio (%)	62	52	15	30	−30
Mean slope (%)	2.4	2.9	2.9	2.6	2.8

Note: Gross erosion and sediment delivery ratio were calculated using the MBM II model. Mean slope values are also shown.

3.1.1 | Plot 1CA0

Plot 1CA0 corresponds to continuous agriculture without fertilizer application in the first LTE block, following a corn–barley/sorghum–wheat/soybean rotation. It showed the highest erosion rates and a steeper slope than plot 2CA0. Unlike the predominantly concave profiles observed across the LTE, the transect displayed an overall flat morphology. A gully cutting diagonally across the plot was identified between 90 and 140 m, with the 120 m point representing the most eroded site among all treatments. At 160 m, ^{137}Cs activity increased with depth, peaking at 20–22.5 cm, consistent with the reference profile. Although the total inventory was lower than the reference, low surface activities indicate deposition of ^{137}Cs-depleted sediments, classifying this point as transitional. At 200 m, ^{137}Cs was detected down to 60 cm, and the inventory exceeded the reference, indicating net sediment accumulation.

3.1.2 | Plot 2CA0

Plot 2CA0 represents the second unfertilized continuous agriculture treatment, under the same crop rotation as plot 1CA0. The transect exhibited a concave profile with an inflection near 160 m transitioning to convex, indicating enhanced erosion. At 5 and 40 m, ^{137}Cs profiles were homogeneous down to 20 cm. Despite the 5 m point showing an inventory higher than the reference, most activity occurred at depth, suggesting downward input rather than surface accumulation. In contrast, the 40 m point had an inventory below the reference and was classified as erosional. At 80 and 120 m, inventories were also below the reference, with the 120 m point being the most eroded along the transect. At 160 m, low surface activity increased to a peak at 22.5 cm before declining, yielding an intermediate inventory and indicating a transitional site. At 200 m, a deep peak at 47.5–50 cm and an inventory exceeding the reference identified this location as a sediment accumulation point.

3.1.3 | Plot CA+

The CA+ plot corresponds to continuous agriculture with mineral fertilization under the same crop rotation as 1CA0 and 2CA0.

This treatment showed moderate erosion, an average slope of 3.0%, and a generally flat profile. Points at 5, 40, and 120 m exhibited inventories below the reference, indicating erosion. Intermediate points at 80 and 160 m showed higher inventories but remained below the reference, classifying them as transitional. At 160 m, the profile was uniform to 15 cm, followed by a secondary peak and decline by 25 cm. At 200 m, a pronounced peak at 50–55 cm and an inventory three times higher than the reference indicated strong sediment accumulation.

3.1.4 | Plot 33%P

Plot 33%P combines crops and pasture (66% crops, 33% pasture) with a red clover–sorghum–wheat/soybean rotation. This treatment exhibited minimal erosion, an average slope of 2.4%, and slight surface soil loss with deposition at the lower end of the transect. Due to its concave profile, the slope direction is reversed over the first 35 m, with the upper point located at 40 m. At 40, 80, and 120 m, ^{137}Cs profiles were similar, with homogeneous activity to 17.5 cm, a peak at 10–15 cm, and a sharp decline below 22.5 cm, consistent with plowed profiles described by Walling and He (1999). Inventories at these points were below the reference, indicating erosion. At 160 m, the profile showed a clear peak at 15–17.5 cm and an inventory exceeding the reference, indicating accumulation. At 200 m, ^{137}Cs reached 35 cm with a peak at 20–22.5 cm, confirming net sediment accumulation at the lower transect positions.

3.1.5 | Plot 50%P

Plot 50%P integrates crops and pasture equally (50%–50%), including three consecutive years of pasture (tall fescue, white clover and birds'-foot trefoil). This treatment showed the highest conservation, with a concave profile and an average slope of 2.8%. At 5 m, the inventory was close to the reference, indicating stability. At 40 m, uniformly elevated ^{137}Cs activity identified sediment accumulation. Points at 80, 120, and 160 m exhibited inventories below the reference, indicating erosion, with the lowest inventory at 160 m. At 200 m, ^{137}Cs was detected down to 40 cm with a peak at 35 cm and an inventory above the reference, confirming sediment accumulation.

3.2 | Comparison of ^{137}Cs Conversion Model Performance With RUSLE

Figure 4 presents erosion rate estimates derived from the ^{137}Cs and RUSLE approaches for selected LTE treatments. Considering all sampling points (left panel), clear treatment-dependent differences are observed, with the highest erosion rates in 1CA0 and 2CA0, supporting the effectiveness of tillage reduction and pasture inclusion in reducing soil erosion (Terra and García-Préchac 2001a; García-Préchac et al. 2004). Differences between ^{137}Cs-derived estimates and RUSLE outputs increase beyond 120 m along the transect, indicating that the two approaches capture different dominant processes as slope length increases. This is consistent with the design of the RUSLE framework based on runoff plots shorter than 120 m (García-Préchac et al. 2016).

RUSLE minimum estimates were consistently lower than RUSLE mean values, and the downslope increase in erosion rates was mainly driven by higher L and S factors. Results of the ^{137}Cs models are consistent with field observations and the process-based point classification, showing strong agreement among models except at two gully-affected sites (1CA0 and 2CA0), where MBM II produced the highest erosion estimates, reflecting differences in model assumptions (Zhang et al. 2015; Zhang 2020).

In the upper transect section (5–80 m; Figure 4, right panel), erosion rates show general agreement within each modeling approach, with modest differences between RUSLE and ^{137}Cs estimates at some locations. Within the CA0 treatment, contrasting responses were observed: RUSLE overestimated erosion in 2CA0 but underestimated it in 1CA0 relative to ^{137}Cs estimates, primarily due to differences in slope and possibly influenced by lateral sediment transport.

At points classified as deposition zones, ^{137}Cs results indicate net sediment accumulation, contrasting with RUSLE outputs. Variability among models increases at these locations, particularly under continuous agriculture. MBM II generally predicted greater deposition than other conversion models, except in the 33%P treatment.

Overall, differences among model outputs reflect contrasting assumptions. RUSLE assumes a single uniform slope aligned with transect management, whereas field observations indicate additional slope components (≈1.9%) producing more complex topography (Figure 1). Moreover, RUSLE estimates only sheet and rill erosion, while ^{137}Cs-based models integrate total soil redistribution. These findings emphasize the need for careful interpretation when comparing ^{137}Cs and RUSLE results, particularly in relation to the sediment process classification of sampling points.

In the forthcoming analysis, the MBM II conversion model was chosen to further study ^{137}Cs, motivated by practical considerations. This model's streamlined parameterization facilitates simpler modeling processes. Preliminary findings demonstrate a strong correlation in erosion values between MBM II and the more complex MBM III. This is particularly evident in the assessment of water erosion redistribution rates, increasing the reliability of the MBM II model.

The scatterplot in Figure 5 organizes data based on erosion points, defined solely by an inventory value lower than the reference, thus including both erosion and transit points (as per the classification in Section 2.6). A noticeable trend of a direct relationship ($R = 0.54$, $n = 21$, $p < 0.01$) between erosion calculated by MBM II and RUSLE is evident. In contrast, accumulation points exhibit an inverse relationship with a well-fitted correlation ($R = -0.95$, $n = 7$, $p < 0.005$).

Further categorization of points based on the criteria (Figure 3) shows a direct relationship exclusively between erosive points and RUSLE outputs ($R = 0.93$, $n = 5$, $p < 0.005$). Points classified as transit maintained a direct trend, albeit with a less linear fit ($R = 0.62$, $n = 16$, $p < 0.01$), underscoring the complexity of soil processes at these points where multiple processes may occur. This intricacy is apparent in the absence

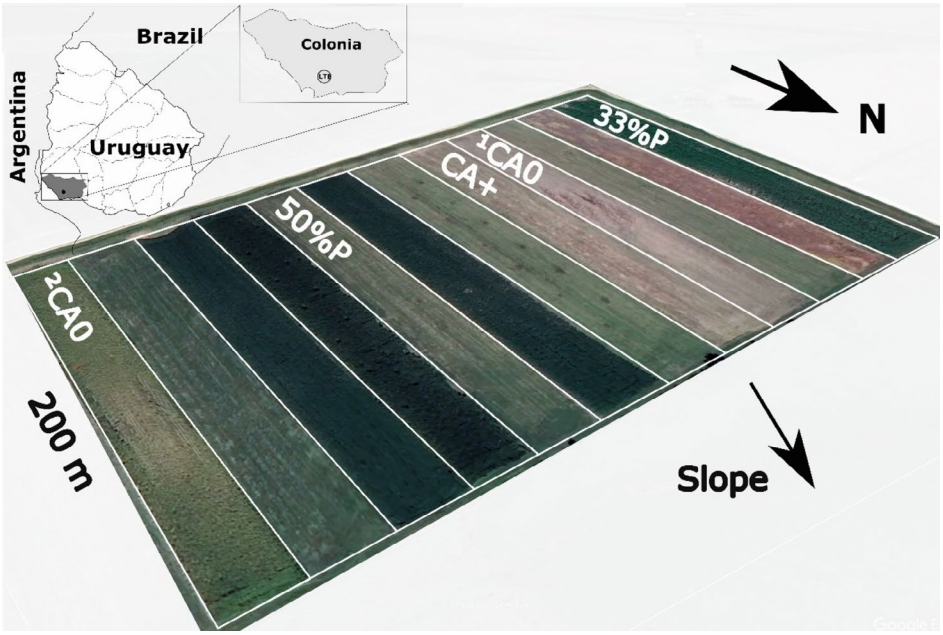

FIGURE 1 | Location and layout of the long-term experiment at La Estanzuela, Uruguay, showing sampled plots. The black arrow indicates the mean slope of the site. Image: Google Earth v7.3.6.9796 2024; CNES/Airbus 2024. [Colour figure can be viewed at wileyonlinelibrary.com]

of a single process influencing soil redistribution processes at these points, where the erosion rate exceeds the sediment deposition rate.

Our findings indicate that ^{137}Cs inventories primarily record erosion occurring shortly after the main fallout period in the 1960s–1970s (Figure 6). More recent soil loss has a reduced imprint on ^{137}Cs inventories because much of the original fallout-derived ^{137}Cs had already been removed or redistributed by earlier erosion events, leaving a depleted soil reservoir.

4 | Discussion

4.1 | Soil Use and Management

4.1.1 | Cropping System

This study provided strong evidence for the key role of CPR in mitigating soil erosion over decades of agricultural activity (Studdert et al. 1997; Wingeyer et al. 2015; Ernst et al. 2018) (Figure 2). Incorporating pastures into rotations improves key soil physical properties (e.g., soil structure, water holding capacity) which contribute to increased water infiltration during intense rainfall events, making soils more resilient to climate change (Altieri et al. 2015; Basche and DeLonge 2019). At this LTE study site, CPR maintained significantly higher SOC levels than continuous agriculture (Grahmann et al. 2020; Rubio et al. 2021). Soil erosion processes are tightly coupled with SOC due to its critical role for soil functions like aggregate stability and porosity (Zhang et al. 2007; Rubio et al. 2021) which explains the lower soil degradation in CPR where SOC was maintained or even enhanced over time. Increasing SOC stocks for climate protection often involves increasing carbon inputs from belowground biomass, particularly from perennial and leguminous pasture roots (Rasse et al. 2005; Martin

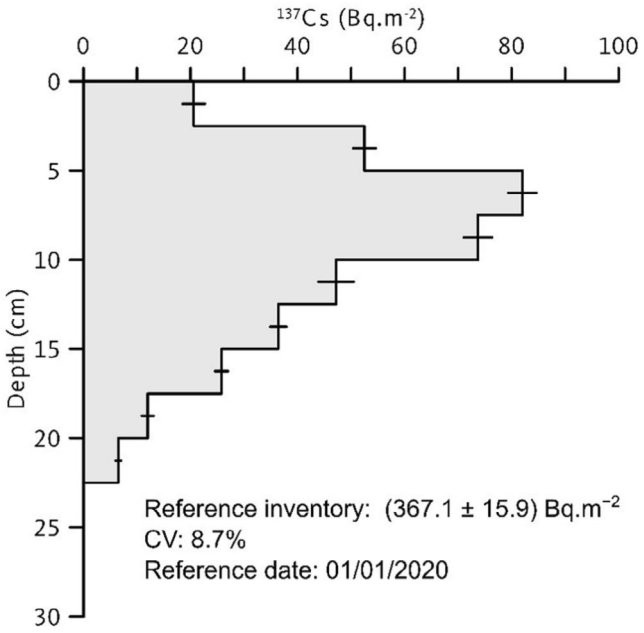

FIGURE 2 | ^{137}Cs depth profile at the reference site, obtained from pooled samples collected every 2.5 cm. The coefficient of variation (CV) was calculated from nine individual samples, and the reference inventory corresponds to their mean. Black horizontal bars indicate uncertainty (Bq m^{-2}).

et al. 2020; Poeplau et al. 2021). Pasture integration has also been show to improve SOC quality, enhancing both the labile and recalcitrant SOC pools when rotated with vegetables (Lin et al. 2020) and total surface soil POM-C and POM-N when rotated with rice (Macedo et al. 2021). On the other hand, it has also been shown for this LTE that adequate fertilization of crops in continuous agriculture decelerates soil degradation compared to unfertilized continues cropping, mainly due to

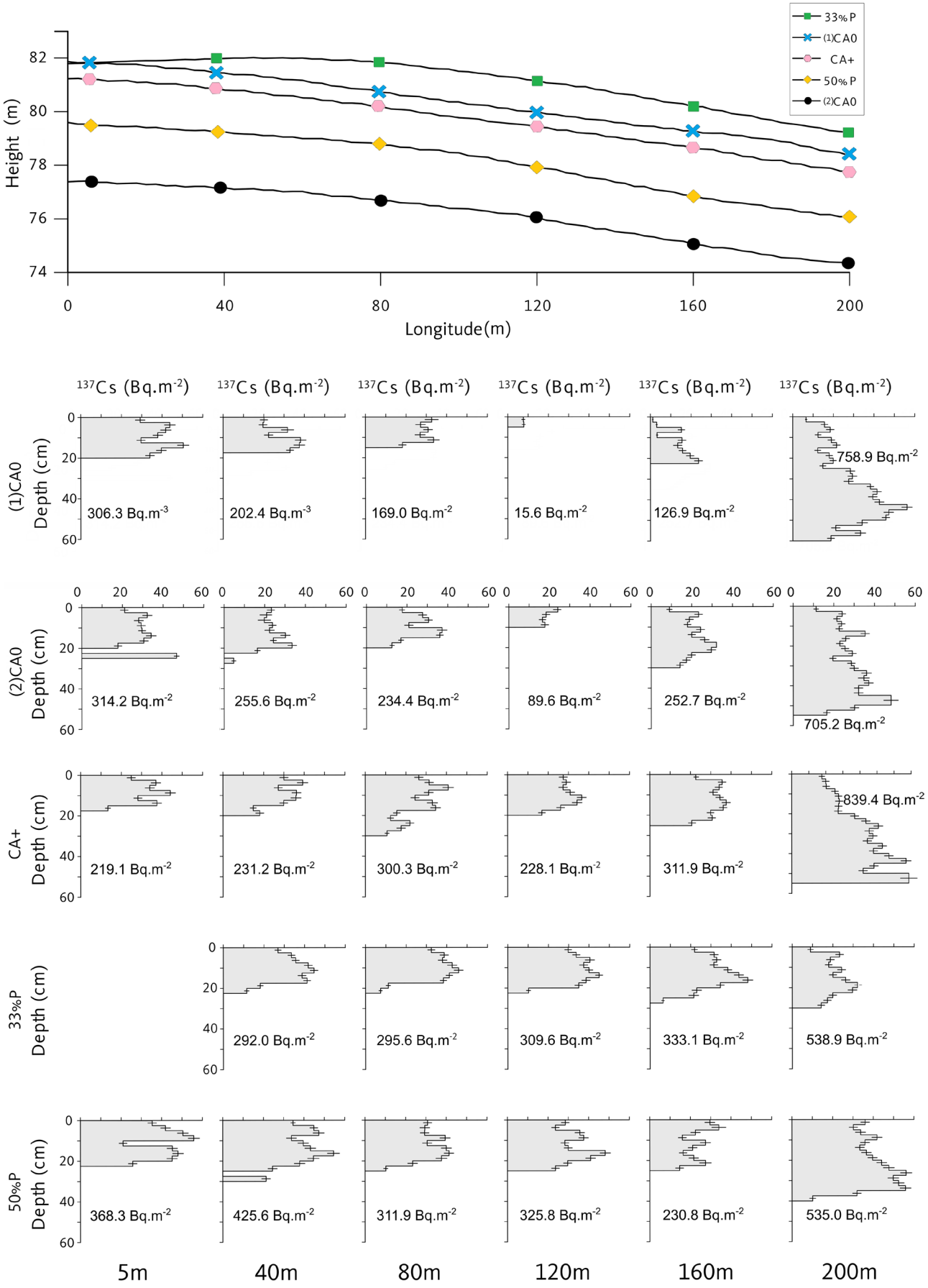

FIGURE 3 | Legend on next page.

FIGURE 3 | Topography (top) and ^{137}Cs total inventory and depth distribution (Bq m^{-2}; bottom) along transects at 5, 40, 80, 120, 160, and 200 m for each plot (continuous agriculture without fertilization in the first (1)CA0 and second block (2)CA0, continuous agriculture with mineral fertilizer application (CA+), crop-pasture rotation (CPR) with 66% crops and 33% pasture (33%P), and CPR with 50% crops and 50% pasture (50%P)). [Colour figure can be viewed at wileyonlinelibrary.com]

higher root biomass production, crop residue cycling and increased soil cover (Rubio et al. 2022).

The selected treatments are categorized into two groups: those incorporating pasture rotations and those without pasture inclusion. It became evident that regardless of the conversion model utilized for estimating erosion based on ^{137}Cs (i.e., MBM II, MBM III or MODERN, (Table S3)), treatments integrating pastures, namely 50%P and 33%P, exhibited a small range of gross erosion from −1.8 to −3.5 Mg ha^{-1} year^{-1} whereas continuous agriculture was notably higher with gross erosion ranging from −14.2 to −17.2 Mg ha^{-1} year^{-1}. This underscores that pasture integration in those plots resulted in a substantial reduction of erosion compared to plots under continuous agriculture and highlights its potential to combat soil erosion in degraded soils (Wingeyer et al. 2015; Tourn et al. 2019). In this way, CPR serves as a mitigation measure to counteract global soil erosion predictions for future climate scenarios (Borrelli et al. 2020).

4.1.2 | ^{137}Cs Depth Profile and Tillage Effects

As illustrated in Figure 3, net erosion dominated across the transects, although localized deposition was observed at discrete sampling points, indicating intra-plot sediment redistribution. Detailed analysis of ^{137}Cs depth distribution profiles revealed that certain mid-slope positions, despite exhibiting lower total inventories relative to the reference site, functioned as transient sediment storage zones rather than true depositional sinks. These locations were characterized by: (i) total ^{137}Cs inventories exceeding those of upslope positions, (ii) depleted surface ^{137}Cs concentrations, and (iii) multiple subsurface activity peaks, collectively indicating episodic sediment deposition. However, the net deficit in ^{137}Cs inventory relative to the reference confirms that sediment export to downslope positions exceeded local sediment input, precluding their classification as net accumulation zones. The occurrence of multiple subsurface ^{137}Cs peaks may also reflect temporal changes in the tillage regime, particularly the transition to no-tillage management since 2009, which restricted soil disturbance to approximately 5 cm depth (García-Préchac et al. 2004), thereby preserving stratified ^{137}Cs signatures from earlier depositional events. Severe erosion culminating in gully formation was particularly pronounced in plots 1CA0 and 2CA0. In plot 1CA0, an active gully at 120 m (Figure 1) was characterized by an extremely depleted ^{137}Cs inventory of 15.6 Bq m^{-2}, indicating near-complete removal of the original soil profile. The replicated treatment 2CA0 exhibited analogous erosive processes at the same distance (120 m), though with a comparatively higher ^{137}Cs inventory of 89.6 Bq m^{-2}. This difference reflects the lower slope gradient in 2CA0, which attenuated erosion rates and delayed gully incision relative to 1CA0.

Additional depth profiles of interest include the 5 m position in treatment 2CA0 and the 40 m position in treatment 50%P (Figure 3), both of which exhibited elevated ^{137}Cs activity in the deepest sampled layer. These subsurface peaks suggest burial of the original ^{137}Cs-enriched topsoil beneath subsequently deposited sediment, providing evidence of substantial localized accumulation at these positions. This phenomenon might be attributed to the direct infiltration of soil with a high concentration of ^{137}Cs, potentially facilitated by cracks formed during the dry season, particularly in expansive soils characterized by large amounts of the smectitic clay type (Liu et al. 2012) as present at the study site.

4.1.3 | Sediment Delivery Ratio

The datasets presented in Figure 4 were integrated with mean sediment yield estimates obtained from mass balance models at the plot outlets (Table S3). Plots with the lowest gross erosion rates corresponded to treatments including pasture, with values of −3.5% and −2.8% for 33%P and 50%P, respectively. This result is consistent with the widely reported erosion-mitigating effect of pasture systems and their role in reducing sediment and nutrient delivery (as sediment enrichment ratio for SOC and total nitrogen) to downstream water bodies (Franzluebbers et al. 2014; Grahmann et al. 2022).

The interpretation of net erosion and sediment redistribution in this study is constrained by the absence of hydrological isolation among plots. In the 50%P treatment, the identified deposition point exhibited a negative sediment delivery ratio, indicating sediment inputs from upslope areas external to the plot. The positive net erosion values further confirm that sediment deposition exceeded in-plot sediment generation (Table 1).

Although 33%P and CA+ displayed similar ^{137}Cs inventories at 80 m and 160 m (Figure 3), CA+ showed higher erosion rates at 40 m and 120 m, resulting in a gross erosion rate approximately twice that of 33%P (Table 1). Despite this contrast, both treatments exhibited identical net erosion rates (−1.1 Mg ha^{-1} year^{-1}), explained by enhanced sediment accumulation at 200 m in CA+ and a lower sediment delivery ratio. While this result appears counterintuitive, given the higher pasture proportion in 33%P, similar slope gradients (2.4% in 33%P and 3.0% in CA+) suggest that topography alone does not account for the observed differences. Instead, the higher deposition observed in CA+ is likely influenced by its downslope position relative to plot 2CA0, which presented the highest sediment export and delivery ratio (Figure 1).

4.2 | Model Comparison and Performance

4.2.1 | RUSLE Mean Versus RUSLE Min

The mean soil erosion rate estimated by RUSLE over the longer time window (1963–1983) was higher (16.1 Mg ha^{-1} year^{-1}) compared to the rate obtained for the most recent period (2009–2020;

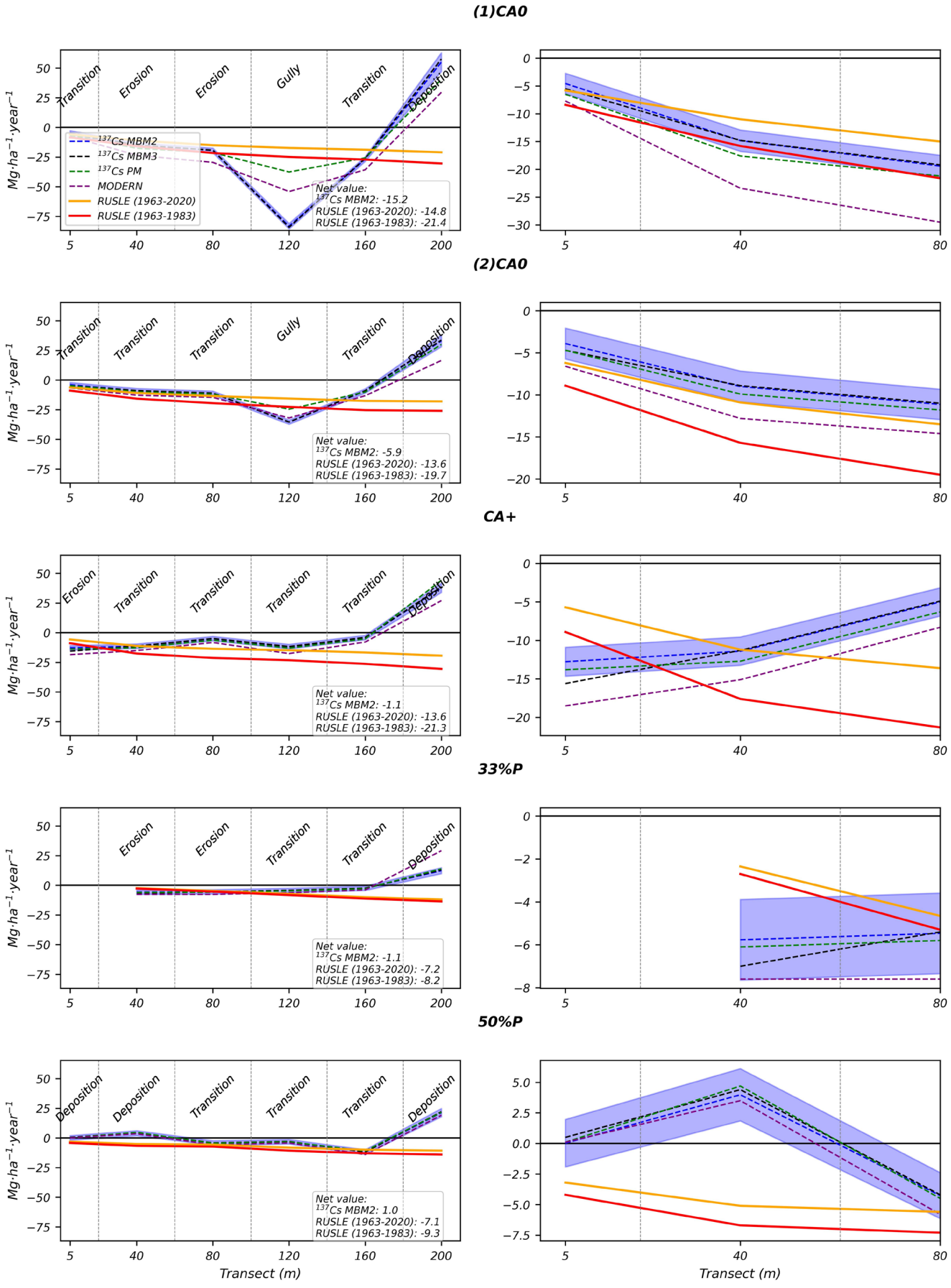

FIGURE 4 | Legend on next page.

FIGURE 4 | Soil redistribution and erosion rates estimated using ^{137}Cs and RUSLE-based models for LTE plots (continuous agriculture without fertilization in the first (1)CA0 and second block (2)CA0, continuous agriculture with mineral fertilizer application (CA+), crop-pasture rotation (CPR) with 66% crops and 33% pasture (33%P), and CPR with 50% crops and 50% pasture (50%P)). The left panel shows all transect points, while the right panel includes only the 5, 40 and 80 m positions. Blue shading indicates the 95% confidence interval of the MBM II model. [Colour figure can be viewed at wileyonlinelibrary.com]

8.65 Mg ha^{-1} year^{-1}) for both CA0 plots. This suggests a potential reduction in soil erosion magnitude in recent decades. The decline in erosion rates aligns with previous findings, indicating that the transition from conventional tillage to no-till practices in the 1990s resulted in lower mean annual erosion rates (Terra and García-Prèchac 2001b). Recent national studies measured yearly average soil losses under 1000 kg ha^{-1} when conservation agriculture principles have been applied (Grahmann et al. 2022), underpinning its effectiveness to control erosion under soil conservation practices using no-till, residue retention and cover crops (Borrelli et al. 2017).

The observed changes in soil erosion cannot be solely explained by land use changes, as cropping practices in the study plots have remained consistent and representative of the region for the past 55–60 years. Given this long-term perspective, the soil erosion rates derived from ^{137}Cs measurements (1963–2020) may partly reflect the impact of climate change, particularly shifts in rainfall patterns. To explore this, *R*-factor values were applied in the RUSLE model using a 20-year moving average, considering both the minimum (Rmin = 3323 MJ mm ha^{-1} h^{-1} year^{-1}) and mean (R mean = 4239 MJ mm ha^{-1} h^{-1} year^{-1}) *R* values per period (Figure 4). Importantly, erosion estimates derived from ^{137}Cs data align more closely with those generated by RUSLE mean, reinforcing the potential impact of changing rainfall intensity over time.

Our results suggest that higher erosivity, reflected by greater R values, aligns better with ^{137}Cs-based erosion models that consider not only water erosion. However, for points primarily affected by erosion (first 40 m), both RUSLE mean and minimum tend to underestimate erosion in CA+ and 2CA0 compared to ^{137}Cs (Figure 4). In contrast, RUSLE overestimated erosion in 50%P. These differences are mainly due to micro-slopes within plots causing localized accumulation or sediment transit (Figures 2 and 4). Therefore, careful criteria are needed when comparing models, focusing on areas where erosion is clearly dominant, specifically sheet and rill erosion, as defined by Renard et al. (1997).

4.2.2 | RUSLE Mean vs. MBM II

The fundamental premise to apply the ^{137}Cs method is that the volume of eroded soil at each sampling point correlates with the extent of ^{137}Cs depletion observed during the period encompassed by the ^{137}Cs measurements (Lizaga Villuendas et al. 2022; Porto and Callegari 2022). Consequently, selecting a conversion model capable of quantifying the reduction in the measured inventory relative to the local reference inventory becomes imperative. The selection of MBM II as the ^{137}Cs conversion model was based on its well-balanced attributes, including simplicity, accuracy, and broad acceptance within the scientific community (Suhartini 2010; Zhang et al. 2015).

In Figure 5, where RUSLE was compared to soil redistribution results of MBM II, we observed a direct relationship of categorical points based exclusively on erosion with RUSLE mean. On the contrary, accumulation points displayed an inverse relationship with a well-fitted correlation which was attributed to the fact that RUSLE predicts higher erosion rates with a longer LS and more intense land use. In turn, MBM II projects greater deposition at lower parts of the slope, resulting from sediment redistribution which was generated in the middle section of the slope due to intensive land use. Those accumulations become more pronounced at this particular study site due to the concave shape of the slope.

The distinction observed between RUSLE and MBM II in Figure 6 could be attributed to the greater sensitivity of ^{137}Cs to historic erosion processes, closely aligned with the period following the fallout of ^{137}Cs. This assumption is supported by the temporal mismatch between the period of maximum soil redistribution, which occurred shortly after the main ^{137}Cs fallout under more intensive soil disturbance conditions, and present-day erosion processes. Contemporary erosion operates on soils where ^{137}Cs inventories have already been substantially modified by prior erosion and redistribution, in combination with ongoing radioactive decay (Porto et al. 2016; Cabrera et al. 2023).

The complex interplay between fallout-derived tracers and landscape dynamics highlights the need for a temporal perspective in interpreting ^{137}Cs inventories, given their sensitivity to both historical and recent erosion. The decay of ^{137}Cs affects present-day erosion assessments, reinforcing the importance of incorporating $^{210}Pb_{ex}$ into studies. As a naturally deposited radionuclide, $^{210}Pb_{ex}$ offers valuable complementary insights, particularly for detecting recent erosive events which are not captured by ^{137}Cs alone (Renard et al. 1997; Porto et al. 2016; Cabrera et al. 2023). Additionally, long-term soil erosion may also benefit from combining repeated topographic surveys with radio-isotopic techniques to refine these estimates.

4.3 | Implications for LTE Management

Over the last decades, LTEs have provided key information regarding sustainable land use, and they will continue to be useful in the future for quantifying and modeling long-term trends in cropping systems (Berti et al. 2016; Baethgen et al. 2021). However, tillage practices over time redistribute the soil and contribute significantly to the within-field (or plot) soil variation in LTEs, affecting SOC, water retention, and bulk density among others (Frye and Thomas 1991). One additional process observed in this study is the lateral contribution of inter-plot sediments, as evidenced by accumulation points at 40 m (Figure 3, 50%P, 40 m point), where exclusively an erosion process would be expected. The arrival of sediments could be due to the fact that the 50%P

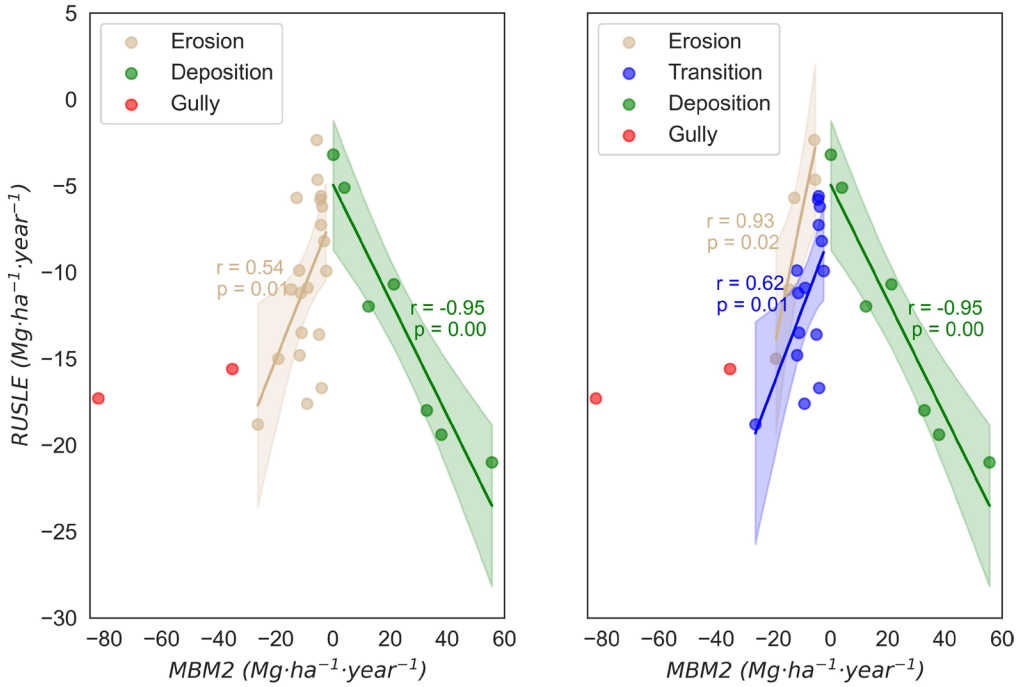

FIGURE 5 | Scatter plots and linear regressions comparing RUSLE mean erosion rates with ^{137}Cs MBM II. The left panel shows a simplified classification grouping erosion and transition points, whereas the right panel uses the full classification described in Section 2.6. [Colour figure can be viewed at wileyonlinelibrary.com]

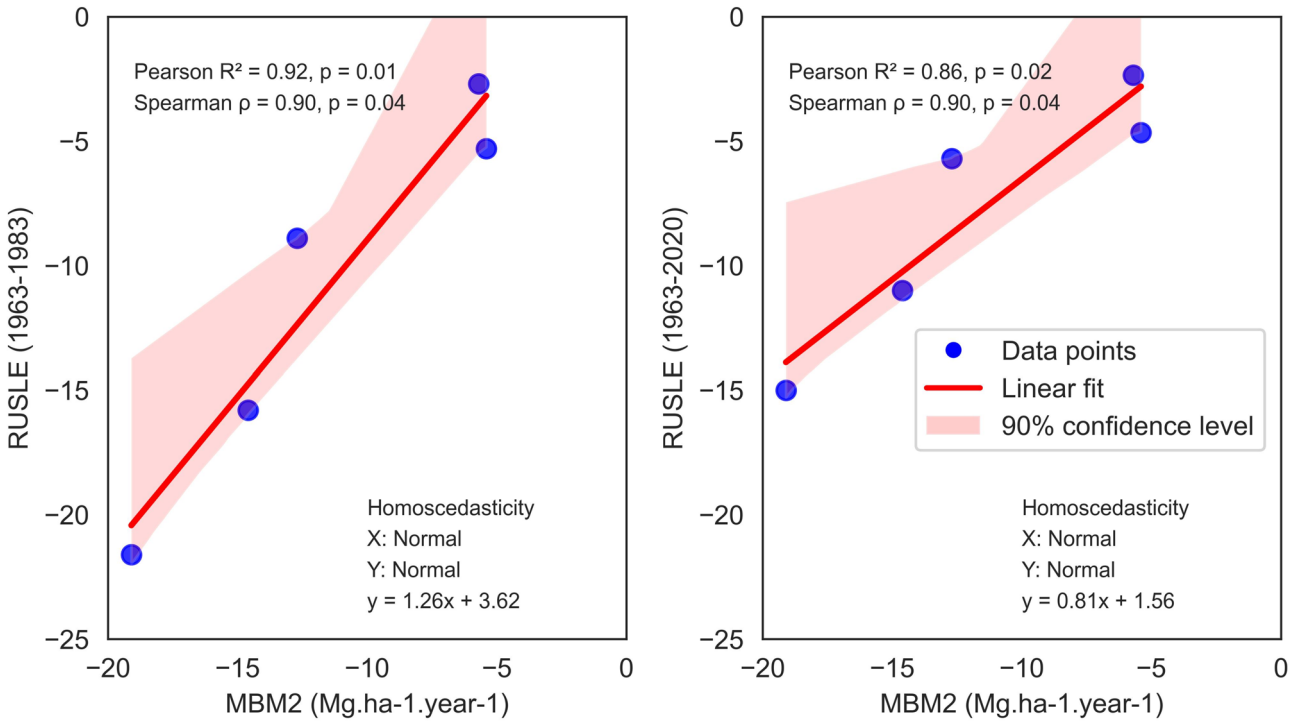

FIGURE 6 | Linear regression analysis comparing RUSLE outputs with the ^{137}Cs MBM II model in the first experimental period from 1963 to 1983 (left) and the entire study period spanning from 1963 to 2020 (right). [Colour figure can be viewed at wileyonlinelibrary.com]

plot is downstream from the 2CA0 plot (Figure 1), which exhibits the highest erosive level and sediment export among all studied plots. Although not the main focus, these results lead to the assumption that horizontal soil displacement can impact LTE soil sampling strategies. Lasting sediment movement between plots may alter observed treatment effects, leading to over- or underestimation of soil–crop responses. Apart from that, yield assessment takes normally place in the plot center, while soil samples are often taken from edges to avoid yield area tramping, and edges are more affected by lateral soil movement, either erosion or deposition. Additionally, in severely eroded plots, current topsoil samples may originate from what was originally the B horizon when the LTE was initiated, affecting interpretation (Grahmann et al. 2020).

5 | Conclusions

The insights of this study contribute to an improved understanding of long-term erosion processes and their manifestation in sedimentary records, thereby facilitating more precise reconstructions of landscape evolution.

This study assessed soil erosion in Uruguay using the ^{137}Cs tracer in the oldest long-term experiment in Latin America, demonstrating the significant impact of agricultural soil management practices on erosion rates. Our results confirmed that continuous cropping systems without fertilization led to a significant increase in soil erosion, while crop-pasture rotations substantially reduced erosion over decades of agricultural production, reinforcing the protective role of pastures.

Evidence from this long-term experiment highlights the critical role of integrated crop-pasture systems in mitigating land degradation processes and reducing soil erosion under temperate agricultural conditions. Results derived from ^{137}Cs inventories and depth profiles clearly show that treatments including pasture consistently exhibited lower gross erosion rates and greater sediment retention than continuous cropping systems, confirming the long-term effectiveness of vegetative cover in controlling soil redistribution.

The comparison between ^{137}Cs-based reconstruction and RUSLE outputs revealed substantial discrepancies, particularly in landscape positions characterized by simultaneous erosion, transport, and deposition processes. In such settings, conventional RUSLE parameterization failed to capture the cumulative soil redistribution observed in the LTE, whereas ^{137}Cs provided an integrated, time-averaged assessment of erosion and sediment connectivity. These results emphasize that a correct differentiation between erosive, transit, and depositional points is essential for reliable erosion estimates in complex agricultural landscapes.

The outcomes of this study are highly relevant to South American agricultural systems, where similar climatic conditions, soil types, and management practices prevail, and where land degradation driven by water erosion remains a major concern. The evidence generated here supports the implementation of public conservation policies that promote crop-pasture rotations as an effective strategy to reduce soil degradation and enhance the long-term sustainability of agricultural production.

Beyond the study area, this research provides a transferable methodological framework for other long-term experiments across South America and temperate cropping systems worldwide. The combined application of fallout radionuclide techniques and erosion models enables a robust evaluation of decadal-scale soil redistribution processes, which is critical for assessing the long-term effectiveness of conservation practices. Future integration of $^{210}Pb_{ex}$ is encouraged to improve sensitivity to more recent erosion dynamics and to further strengthen land degradation assessments in long-term experiments.

Author Contributions

Marcos Tassano: conceptualization, sampling, sample processing, gamma spectrometry measurements, data curation, formal analysis, investigation, methodology, resources, visualization, writing – original draft, writing – review and editing. **Mirel Cabrera:** conceptualization, sampling, sample processing, gamma spectrometry measurements, data curation, formal analysis, investigation, methodology, resources, visualization, writing – original draft, writing – review and editing. **Joan Gonzalez:** sampling, sample processing, gamma spectrometry measurements, investigation, methodology, writing – original draft, writing – review and editing. **Mario Perez-Bidegain:** RUSLE modeling, writing – review and editing. **Olivier Evrard:** writing – review and editing. **Kathrin Grahmann:** conceptualization, writing – original draft, writing – review and editing, funding acquisition. **J. Andrés Quincke:** conceptualization, funding acquisition, sampling, writing – review and editing.

Acknowledgments

We thank Emiliano Barolín and Héctor Vergara for field work support and Lucia Gonzalez for gamma spectrometry measurements support. INIA provided sustained support for keeping soil management and cropping practices in accordance with treatment definitions of this long-term experiment. Open Access funding enabled and organized by Projekt DEAL.

Funding

This project was funded by the Fondo María Viñas (FMV_1_2019_1_156244) and an ANII graduate fellowship granted to J.G. (POS_FMV_2020_1_1009251). K.G. acknowledges financial support from BMFTR for the Junior Research Group SoilRob, project ID 031B1391. M.T., M.C., and O.E. acknowledge the support of the "CELESTE lab" Climat-AMSUD project, funded by ANII (Uruguay) ID: MOV_CO_2023_1_1012408. We thank the graduate program "PEDECIBA Geociencias" for their support in the postgraduate studies of J.G.

Conflicts of Interest

The authors declare no conflicts of interest.

Data Availability Statement

The data that support the findings of this study are available from the corresponding author upon reasonable request.

Endnotes

[1] Open license is governed by the "Licencia de Datos Abiertos – Uruguay" from the "Agencia de Gobierno Electrónico y Sociedad de la Información y del Conocimiento" (Agesic).

References

Alewell, C., P. Borrelli, K. Meusburger, and P. Panagos. 2019. "Using the USLE: Chances, Challenges and Limitations of Soil Erosion Modelling." *International Soil and Water Conservation Research* 7: 203–225. https://doi.org/10.1016/j.iswcr.2019.05.004.

Alonso, J., P. Audicio, L. Martinez, M. Scavone, and E. Rezzano. 2012. "Comparison of Measured 137Cs Data and USLE/RUSLE Simulated Long-Term Erosion Rates." *Agrociencia* 16: 261–267. https://doi.org/10.31285/agro.16.681.

Altamirano, A., H. Da Silva, A. Durán, A. Echevarría, D. Panario, and R. Puentes. 1976. "Carta de Reconocimiento de Suelos del Uruguay a Escala 1:1.000.000."

Altieri, M. A., C. I. Nicholls, A. Henao, and M. A. Lana. 2015. "Agroecology and the Design of Climate Change-Resilient Farming Systems." *Agronomy for Sustainable Development* 35: 869–890. https://doi.org/10.1007/s13593-015-0285-2.

Arata, L., K. Meusburger, E. Frenkel, et al. 2016. "Modelling Deposition and Erosion Rates With RadioNuclides (MODERN) - Part 1: A New Conversion Model to Derive Soil Redistribution Rates From Inventories of Fallout Radionuclides." *Journal of Environmental Radioactivity* 162: 45–55. https://doi.org/10.1016/j.jenvrad.2016.05.008.

Baethgen, W. E., W. J. Parton, V. Rubio, R. H. Kelly, and S. Lutz. 2021. "Ecosystem Dynamics of Crop–Pasture Rotations in a Fifty-Year Field Experiment in Southern South America: Century Model and Field Results." *Soil Science Society of America Journal* 85: 423–437. https://doi.org/10.1002/saj2.20204.

Basche, A. D., and M. S. DeLonge. 2019. "Comparing Infiltration Rates in Soils Managed With Conventional and Alternative Farming Methods: A Meta-Analysis." *PLoS One* 14: 1–22. https://doi.org/10.1371/journal.pone.0215702.

Berti, A., A. D. Marta, M. Mazzoncini, and F. Tei. 2016. "An Overview on Long-Term Agro-Ecosystem Experiments: Present Situation and Future Potential." *European Journal of Agronomy* 77: 236–241. https://doi.org/10.1016/j.eja.2016.01.004.

Borrelli, P., D. A. Robinson, L. R. Fleischer, et al. 2017. "An Assessment of the Global Impact of 21st Century Land Use Change on Soil Erosion." *Nature Communications* 8: 1–8. https://doi.org/10.1038/s41467-017-02142-7.

Borrelli, P., D. A. Robinson, P. Panagos, et al. 2020. "Land Use and Climate Change Impacts on Global Soil Erosion by Water (2015-2070)." *Proceedings of the National Academy of Sciences of the United States of America* 117: 21994–22001. https://doi.org/10.1073/pnas.2001403117.

Cabrera, M., R. Sanabria, J. González, et al. 2023. "Using 137Cs and 210Pbex to Assess Soil Redistribution at Different Temporal Scales Along With Lithogenic Radionuclides to Evaluate Contrasted Watersheds in the Uruguayan Pampa Grassland." *Geoderma* 435: 116502. https://doi.org/10.1016/j.geoderma.2023.116502.

Cayssials, R., J. Liesegang, and J. Piñeyrúa. 1978. "Panorama de la Erosión y Conservación de Suelos en Uruguay, Boletín Técnico No. 4."

Chaboche, P. A., F. Pointurier, P. Sabatier, et al. 2022. "240Pu/239Pu Signatures Allow Refining the Chronology of Radionuclide Fallout in South America." *Science of the Total Environment* 843: 156943. https://doi.org/10.1016/j.scitotenv.2022.156943.

Chaboche, P. A., N. P. A. Saby, J. P. Laceby, et al. 2021. "Mapping the Spatial Distribution of Global 137Cs Fallout in Soils of South America as a Baseline for Earth Science Studies." *Earth-Science Reviews* 214: 103542. https://doi.org/10.1016/j.earscirev.2021.103542.

Chen, P., M. Czymzik, Z. Yu, et al. 2023. "Tendency of Soil Erosion Dynamics by Coupling Radioisotopes and RUSLE Model on the Southeastern Tibetan Plateau in Response to Climate Warming and Human Activity." *Catena* 223: 106954. https://doi.org/10.1016/j.catena.2023.106954.

Čupić, A., I. Smičiklas, M. Manić, et al. 2025. "137Cs-Based Assessment of Soil Erosion Rates in a Morphologically Diverse Catchment With Varying Soil Types and Vegetation Cover: Relationship With Soil Properties and RUSLE Model Predictions." *Water* 17: 526. https://doi.org/10.3390/w17040526.

Dell'Acqua, M., and A. Beretta-Blanco. 2020. "Estimación Del Impacto de la Implementación de la Política de Planes de Uso y Manejo Responsable Del Suelo en la Reducción de las Pérdidas de Los Suelos por Erosión Hídrica."

Ernst, O., and G. Siri-Prieto. 2009. "Impact of Perennial Pasture and Tillage Systems on Carbon Input and Soil Quality Indicators." *Soil and Tillage Research* 105: 260–268. https://doi.org/10.1016/j.still.2009.08.001.

Ernst, O. R., S. Dogliotti, M. Cadenazzi, and A. R. Kemanian. 2018. "Shifting Crop-Pasture Rotations to No-Till Annual Cropping Reduces Soil Quality and Wheat Yield." *Field Crops Research* 217: 180–187. https://doi.org/10.1016/j.fcr.2017.11.014.

FAO. 2019. "Global Symposium on Soil Erosion, Outcome Doc."

FAO, IUSS Working Group WRB. 2022. *World Reference Base for Soil Resources. International Soil Classification System for Naming Soils and Creating Legends for Soil Maps*. 4th ed. International Union of Soil Sciences (IUSS).

Foucher, A., M. Tassano, P. A. Chaboche, et al. 2023. "Inexorable Land Degradation due to Agriculture Expansion in South American Pampa." *Nature Sustainability* 6: 662–670. https://doi.org/10.1038/s41893-023-01074-z.

Franzluebbers, A. J., and F. Gastal. 2018. "Building Agricultural Resilience With Conservation Pasture-Crop Rotations." In *Agroecosystem Diversity: Reconciling Contemporary Agriculture and Environmental Quality*, 109–121. Elsevier Inc. https://doi.org/10.1016/B978-0-12-811050-8.00007-8.

Franzluebbers, A. J., J. Sawchik, and M. A. Taboada. 2014. "Agronomic and Environmental Impacts of Pasture-Crop Rotations in Temperate North and South America." *Agriculture, Ecosystems & Environment* 190: 18–26. https://doi.org/10.1016/j.agee.2013.09.017.

Frye, W. W., and G. W. Thomas. 1991. "Management of Long-Term Field Experiments." *Agronomy Journal* 83: 38–44. https://doi.org/10.2134/agronj1991.00021962008300010012x.

García-Préchac, F., C. Clérici, M. Hill, and E. Hill. 2016. *EROSION Versión 6.0.20: Programa de Computación Para Usar USLE/RUSLE en la Región Sur de la Cuenca Del Plata*, 1–14. Faculty of Agronomy-UdelaR.

García-Préchac, F., and A. Durán. 1998. "Propuesta de Estimación Del Impacto de la Erosión Sobre la Productividad Del Suelo Del Uruguay." *Agrociencia* 1, no. 2: 26–36.

García-Préchac, F., O. Ernst, G. Siri-Prieto, and J. A. Terra. 2004. "Integrating No-Till Into Crop-Pasture Rotations in Uruguay." *Soil & Tillage Research* 77: 1–13. https://doi.org/10.1016/j.still.2003.12.002.

García-Préchac, F., J. Terra, J. Sawchik, and M. Pérez-Bidegain. 2017. "Mejora de Las Estimaciones Con USLE/RUSLE Empleando Resultados de Parcelas de Escurrimiento Para Considerar el Efecto Del Agua Del Suelo." *Agrociencia Uruguay* 21: 100–104. https://doi.org/10.2477/vol21iss2pp100-104.

García-Ruiz, J. M., S. Beguería, E. Nadal-Romero, J. C. González-Hidalgo, N. Lana-Renault, and Y. Sanjuán. 2015. "A Meta-Analysis of Soil Erosion Rates Across the World." *Geomorphology* 239: 160–173. https://doi.org/10.1016/j.geomorph.2015.03.008.

Gharbi, F., T. H. Alsheddi, R. B. Ammar, and M. A. El-Naggar. 2020. "Combination of 137cs and 210pb Radioactive Atmospheric Fallouts to Estimate Soil Erosion for the Same Time Scale." *International Journal of Environmental Research and Public Health* 17: 1–8. https://doi.org/10.3390/ijerph17228292.

Grahmann, K., V. Rubio Dellepiane, J. A. Terra, and J. A. Quincke. 2020. "Long-Term Observations in Contrasting Crop-Pasture Rotations Over Half a Century: Statistical Analysis of Chemical Soil Properties and Implications for Soil Sampling Frequency." *Agriculture, Ecosystems & Environment* 287: 106710. https://doi.org/10.1016/j.agee.2019.106710.

Grahmann, K., V. Rubio, M. Perez-bidegain, and J. A. Quincke. 2022. "Soil Use Legacy as Driving Factor for Soil Erosion Under Conservation Agriculture." *Frontiers in Environmental Science* 10: 1–15. https://doi.org/10.3389/fenvs.2022.822967.

Harris, C. R., K. J. Millman, S. J. van der Walt, et al. 2020. "Array Programming With NumPy." *Nature* 585: 357–362. https://doi.org/10.1038/s41586-020-2649-2.

He, Q., and D. E. Walling. 1997. "The Distribution of Fallout 137Cs and 210Pb in Undisturbed and Cultivated Soils." *Applied Radiation and Isotopes* 48: 677–690. https://doi.org/10.1016/S0969-8043(96)00302-8.

Hunter, J. D. 2007. "Matplotlib: A 2D Graphics Environment." *Computer Science & Engineering* 9: 90–95. https://doi.org/10.1109/MCSE.2007.55.

Lin, D., R. L. McCulley, J. A. Nelson, K. L. Jacobsen, and D. Zhang. 2020. "Time in Pasture Rotation Alters Soil Microbial Community Composition and Function and Increases Carbon Sequestration Potential in a Temperate Agroecosystem." *Science of the Total Environment* 698: 134233. https://doi.org/10.1016/j.scitotenv.2019.134233.

Liu, X., C. Lee Burras, Y. S. Kravchenko, et al. 2012. "Overview of Mollisols in the World: Distribution, Land Use and Management." *Canadian Journal of Soil Science* 92: 383–402. https://doi.org/10.4141/CJSS2010-058.

Lizaga Villuendas, I., B. Latorre, L. Gaspar, and A. Navas. 2022. "Effect of Historical Land-Use Change on Soil Erosion in a Mediterranean Catchment by Integrating 137 cs Measurements and WaTEM/SEDEM Model." *Hydrological Processes* 36: e14577. https://doi.org/10.1002/hyp.14577.

Macedo, I., M. V. Pravia, J. Castillo, and J. A. Terra. 2021. "Soil Organic Matter in Physical Fractions After Intensification of Irrigated Rice-Pasture Rotation Systems." *Soil & Tillage Research* 213: 105160. https://doi.org/10.1016/j.still.2021.105160.

Martin, G., J. L. Durand, M. Duru, et al. 2020. "Role of Ley Pastures in Tomorrow's Cropping Systems. A Review." *Agronomy for Sustainable Development* 40: 17. https://doi.org/10.1007/s13593-020-00620-9.

McKinney, W. 2010. "Data Structures for Statistical Computing in Python." In *Proceedings of the 9th Python in Science Conference 2010*, 51–56. https://doi.org/10.25080/Majora-92bf1922-00a.

MGAP-MVOTMA. 2005. Plan de Acción Nacional de lucha contra la Desertificación y la Sequía. Ministerio de Ganadería, Agricultura y Pesca, Ministerio de Vivienda, Ordenamiento Territorial y Medio Ambiente Proyecto GM2/020/CCD. Montevideo. http://www.mgap.gub.uy/renare.

Pérez Bidegain, M., J. M. Piaggio, W. Baethgen, and F. García Préchac. 2022. "Rainfall Erosivity Factor Update in Uruguay." *Agrociencia Uruguay* 26: 10.31285/AGRO.26.1074.

Perez-Bidegain, M., M. Hill, C. Clerici, et al. 2018. "Regulatory Utilization of USLE/RUSLE Erosion Rate Estimates in Uruguay: A Policy Coincident With the UN Sustainable Development Goals." In *Soil and Sustainable Development Goal*, edited by R. Lal, R. Horn, and T. Kosaki, 82–91. Catena Soil Sciences - Schweizerbart.

Poeplau, C., A. Don, and F. Schneider. 2021. "Roots Are Key to Increasing the Mean Residence Time of Organic Carbon Entering Temperate Agricultural Soils." *Global Change Biology* 27: 4921–4934. https://doi.org/10.1111/gcb.15787.

Porto, P., M. Bacchi, G. Preiti, M. Romeo, and M. Monti. 2022. "Combining Plot Measurements and a Calibrated RUSLE Model to Investigate Recent Changes in Soil Erosion in Upland Areas in Southern Italy." *Journal of Soils and Sediments* 22: 1010–1022. https://doi.org/10.1007/s11368-021-03119-2.

Porto, P., and G. Callegari. 2022. "Comparing Long-Term Observations of Sediment Yield With Estimates of Soil Erosion Rate Based on Recent 137Cs Measurements. Results From an Experimental Catchment in Southern Italy." *Hydrological Processes* 36: 10.1002/hyp.14663.

Porto, P., D. E. Walling, V. Cogliandro, and G. Callegari. 2016. "Exploring the Potential for Using 210Pbex Measurements Within a Re-Sampling Approach to Document Recent Changes in Soil Redistribution Rates Within a Small Catchment in Southern Italy." *Journal of Environmental Radioactivity* 164: 158–168. https://doi.org/10.1016/j.jenvrad.2016.06.026.

Rasse, D. P., C. Rumpel, and M. F. Dignac. 2005. "Is Soil Carbon Mostly Root Carbon? Mechanisms for a Specific Stabilisation." *Plant and Soil* 269: 341–356. https://doi.org/10.1007/s11104-004-0907-y.

Raybaut, P. 2009. "Spyder-Documentation." Pythonhosted.org.

Renard, K., G. Foster, G. Weesies, D. McCool, and D. Yoder. 1997. *Predicting Soil Erosion by Water: A Guide to Conservation Planning With the Revised Universal Soil Loss Equation (RUSLE)*. US Department of Agriculture, Agricultural Research Service, Agriculture Handbook Number 703.

Renard, K. G., G. R. Foster, G. A. Weesies, and J. P. Porter. 1991. "RUSLE: Revised Universal Soil Loss Equation." *Journal of Soil and Water Conservation* 46: 30–33.

Ritchie, J. C., and P. E. Rasmussen. 2000. "Application of 137cesium to Estimate Erosion Rates for Understanding Soil Carbon Loss on Long-Term Experiments at Pendleton, Oregon." *Land Degradation & Development* 11: 75–81. https://doi.org/10.1002/(sici)1099-145x(200001/02)11:1<75::aid-ldr379>3.0.co;2-0.

Rubio, V., R. Diaz-Rossello, J. A. Quincke, and H. M. van Es. 2021. "Quantifying Soil Organic Carbon's Critical Role in Cereal Productivity Losses Under Annualized Crop Rotations." *Agriculture, Ecosystems and Environment* 321: 107607. https://doi.org/10.1016/j.agee.2021.107607.

Rubio, V., J. Sawchik, and H. M. van Es. 2022. "Soil Health Benefits From Sequence Intensification, Fertilization, and No-Tillage in Annual Cropping Systems." *Soil Security* 9: 100074. https://doi.org/10.1016/j.soisec.2022.100074.

Smith, P. 2004. "How Long Before a Change in Soil Organic Carbon Can Be Detected?" *Global Change Biology* 10: 1878–1883. https://doi.org/10.1111/j.1365-2486.2004.00854.x.

Soil Survey Staff. 2022. *Keys to Soil Taxonomy*. 13th ed. USDA Natural Resources Conservation Service.

Soto, J., and A. Navas. 2008. "A Simple Model of cs-137 Profile to Estimate Soil Redistribution in Cultivated Stony Soils." *Radiation Measurements* 43: 1285–1293. https://doi.org/10.1016/j.radmeas.2008.02.024.

Studdert, G. A., H. E. Echeverría, and E. M. Casanovas. 1997. "Crop-Pasture Rotation for Sustaining the Quality and Productivity of a Typic Argiudoll." *Soil Science Society of America Journal* 61: 1466. https://doi.org/10.2136/sssaj1997.03615995006100050026x.

Suhartini, N. 2010. "The Influence of Conversion Model Choice for Erosion Rate Estimation and the Sensitivity of the Results to Changes in the Model Parameter." *Indian Journal of Chemistry* 6: 199–204. https://doi.org/10.22146/ijc.21761.

Tassano, M., P. Cabral, and M. Cabrera. 2025. "Inventory of Cesium-137 and Lead-210 in Reference Soils From the Center-West of Uruguay: Baseline for Erosion Studies and Radiological Monitoring." *INNOTEC* 29: e682. https://doi.org/10.26461/29.06.

Tassano, M., A. Montañez, L. Nuñez, et al. 2021. "Spatial Cross-Correlation Between Physicochemical and Microbiological Variables at Superficial Soil With Different Levels of Degradation." *Catena* 198: 105000. https://doi.org/10.1016/j.catena.2020.105000.

Terra, J., and F. García-Préchac. 2001a. "Evolucion de Indicadores de Calidad de Suelos en Sistemas Forrajeros Con Siembra Directa." In *Reunión Técnica Sobre Siembra Directa, 2001 Memorias*, 40–41. INIA Carillanca/PROCISUR, Las Brujas, Canelones.

Terra, J., and F. García-Prèchac. 2001b. "Efecto de la Intensidad de Uso y Laboreo Sobre el Recurso Suelo y su Calidad." In *Siembra Directa y Rotaciones Forrajeras en las Lomadas del Este: Síntesis 1995–2000*, 8–33. INIA Serie Técnica.

Tourn, S. N., C. C. Videla, and G. A. Studdert. 2019. "Ecological Agriculture Intensification Through Crop-Pasture Rotations Does Improve Aggregation of Southeastern-Pampas Mollisols." *Soil and Tillage Research* 195: 104411. https://doi.org/10.1016/j.still.2019.104411.

Virtanen, P., R. Gommers, T. E. Oliphant, et al. 2020. "SciPy 1.0 Contributors. SciPy 1.0: Fundamental Algorithms for Scientific Computing in Python." *Nature Methods* 17, no. 3: 261–272.

Walling, D. E., and Q. He. 1999. "Improved Models for Estimating Soil Erosion Rates From Cesium-137 Measurements." *Journal of*

Environmental Quality 28: 611–622. https://doi.org/10.2134/jeq1999.00472425002800020027x.

Walling, D. E., Q. He, and P. Appleby. 2002. "G.: Conversion Models for Use in Soil-Erosion, Soil-Redistribution and Sedimentation Investigations." In *Handbook for the Assessment of Soil Erosion and Sedimentation Using Environmental Radionuclides*, 111–164. Kluwer Academic Publishers. https://doi.org/10.1007/0-306-48054-9_7.

Walling, D. E., P. Porto, Y. Zhang, and P. Du. 2014. "Upscaling the Use of Fallout Radionuclides in Soil Erosion and Sediment Budget Investigations: Addressing the Challenge." *International Soil and Water Conservation Research* 2: 1–21. https://doi.org/10.1016/S2095-6339(15)30019-8.

Walling, D. E., Y. Zhang, and Q. He. 2011. "Models for Deriving Estimates of Erosion and Deposition Rates From Fallout Radionuclide (Caesium-137, Excess Lead-210, and Beryllium-7) Measurements and the Development of User-Friendly Software for Model Implementation." In *Impact of Soil Conservation Measures on Erosion Control and Soil Quality*, 11–34. IAEA-TECDO.

Wingeyer, A. B., T. J. C. Amado, M. Pérez-Bidegain, et al. 2015. "Soil Quality Impacts of Current South American Agricultural Practices." *Sustainability* 7: 2213–2242. https://doi.org/10.3390/su7022213.

Wischmeier, W. H., and D. D. Smith. 1978. "Predicting Rainfall Erosion Losses: A Guide to Conservation Planning, Department of Agriculture." *Science and Education Administration* 58: 7250–7257. https://doi.org/10.1128/AAC.03728-14.

Zapata, F. 2003. "The Use of Environmental Radionuclides as Tracers in Soil Erosion and Sedimentation Investigations: Recent Advances and Future Developments." *Soil and Tillage Research* 69: 3–13. https://doi.org/10.1016/S0167-1987(02)00124-1.

Zhang, G. S., K. Y. Chan, A. Oates, D. P. Heenan, and G. B. Huang. 2007. "Relationship Between Soil Structure and Runoff/Soil Loss After 24 Years of Conservation Tillage." *Soil and Tillage Research* 92: 122–128. https://doi.org/10.1016/j.still.2006.01.006.

Zhang, X. C. (J.). 2020. "Dynamic Depth Distribution of Cesium-133 Near Soil Surfaces in Packed Soils Under Multiple Simulated Rains." *Catena* 194: 104710. https://doi.org/10.1016/j.catena.2020.104710.

Zhang, X. C. (J.), G. H. Zhang, and X. Wei. 2015. "How to Make 137Cs Erosion Estimation More Useful: An Uncertainty Perspective." *Geoderma* 239–240: 186–194. https://doi.org/10.1016/j.geoderma.2014.10.004.

Zurbriggen, C., M. González-Lago, M. Baraibar, W. Baethgen, N. Mazzeo, and M. Sierra. 2020. "Experimentation in the Design of Public Policies: The Uruguayan Soils Conservation Plans." *Iberoamericana – Nordic Journal of Latin American and Caribbean Studies* 49: 52–62. https://doi.org/10.16993/iberoamericana.459.

Supporting Information

Additional supporting information can be found online in the Supporting Information section. **Data S1:** ldr70498-sup-0001-Supinfo.docx.